Electronic Supplementary Information

for

Reactivity of a Ru(III)-hydroxo complex in substrate oxidations in water

*Shingo Ohzu, Tomoya Ishizuka, Hiroaki Kotani, and Takahiko Kojima**

Department of Chemistry, Faculty of Pure and Applied Sciences, University of Tsukuba,

1-1-1 Tennoudai, Tsukuba, Ibaraki 305-8571, Japan

General.

Chemicals and solvents were used as received from Tokyo Chemical Industry (TCI) Co., Wako chemicals, or Sigma-Aldrich Corp. unless otherwise mentioned. $PY5Me_2$ was synthesized with a modified procedure reported in literature (*vide infra*).[1] UV-vis spectra were collected on a Shimadzu UV-3600 spectrophotometer, equipped with a temperature-controller, UNISOK UnispeKs. ^1H NMR spectra were recorded on JEOL EX-270 and JNM-ECS 400 spectrometers at room temperature and the chemical shifts of signals were determined with respect to residual proton signals of deuterated solvents. Electrochemical measurements were performed with a BAS CV-1B electrochemical analyser and an AUTOLAB PGSTAT12 potentiometer in Britton-Robinson (B.-R.) buffer (pH = 2~12) at room temperature. pH measurements were made using a Horiba pH-Meter F-51. Stopped-flow measurements were performed with a UNISOKU RSP-2000 stopped-flow spectrophotometer.

Synthesis of $[Ru^{II}Cl(PY5Me_2)](PF_6)$. The ethanol solution (50 mL) containing $PY5Me_2$[1] (91 mg, 0.2 mmol) and $RuCl_3 \cdot 3H_2O$ (65 mg, 0.25 mmol) was refluxed under Ar atmosphere for 24 h. After cooling to room temperature, the solvent was completely removed and the resultant yellow solid was dissolved in water. Upon addition of excess amount of NH_4PF_6, yellow solid emerged and the precipitate was filtered and washed with diethyl ether to remove organic impurities. Yield: 60 mg (41%). ESI-MS (methanol): m/z = 504 ($[M - PF_6]^+$). Anal. Calcd for $C_{29}H_{25}N_5RuClPF_6$: C, 48.85; H, 3.96; N, 9.18. Found: C, 48.68; H, 4.08; N, 9.16. UV-Vis (CH_3CN): λ_{max} [nm] = 395, 351, 248. ^1H NMR (δ in CD_3CN, 400 MHz): 2.73 (s, 6H, Me), 7.41 (dd, J = 6, 2 Hz, 4H, H5 of Py_{side}), 7.84 (m, 5H, H4 of Py_{centre} and H4 of Py_{side}), 7.93 (m, 6H, H3 of Py_{centre} and H3 of Py_{side}), 9.67 (d, J = 6 Hz, 4H, H6 of Py_{side}).

Synthesis of $[Ru^{II}(PY5Me_2)(OH_2)](PF_6)_2$ (1). An H_2O solution (40 mL) containing $[RuCl(PY5Me_2)](PF_6)$ (58 mg, 80 μmol) and $AgPF_6$ (24 mg, 96 μmol) was refluxed for 3 h. Insoluble white solid was removed by a membrane filter (ADVANTEC H100A025A), and then the solvent of the filtrate was concentrated to a 1/10 volume to obtain a yellow precipitate. The yellow precipitate was recrystallized from a minimal amount of warmed H_2O. The resulting yellow powder was filtered, and dried *in vacuo*. Yield: 35 mg (52%). ESI-MS (methanol): m/z = 281 ($[M - H_2O - 2PF_6 + N_2]^{2+}$). Anal. Calcd (%) for $C_{29}H_{25}N_5ORuP_2F_{12}$: C, 40.85; H, 3.19; N, 8.21. Found: C, 40.89; H, 3.11; N, 8.40. UV-Vis (H_2O): λ_{max} [nm] = 381, 246. ^1H NMR (δ in D_2O, 400 MHz): 2.84 (s, 6H, Me), 7.52 (dd, J = 6, 2 Hz, 4H, H5 of Py_{side}), 7.96 (m, 5H, H4 of Py_{centre} and H4 of Py_{side}), 8.05 (m, 6H, H3 of Py_{centre} and H3 of Py_{side}), 9.41 (d, J = 6 Hz, 4H, H6 of Py_{side}).

Synthesis of $[Ru^{III}(OH)(PY5Me_2)](PF_6)_2$ (2). The Ru^{III}-OH complex **2** was formed by the electrochemical oxidation of **1** (0.5 mM, 2ml) at +1.3 V (vs SCE) in B.-R. buffer solution (pH 1.8) for *ca*. 30 min. ESI-MS (H_2O): m/z = 281.2 ($[M - 2PF_6]^{2+}$). UV-vis (H_2O): λ_{max} [nm] = 262.

X-ray Crystallography on $[Ru^{II}Cl(PY5Me_2)](PF_6)$.

A single crystal of $[Ru^{II}Cl(PY5Me_2)](PF_6)$ was obtained through recrystallization by the vapour diffusion of ethyl acetate into the methanol solution of $[Ru^{II}Cl(PY5Me_2)](PF_6)$. Diffraction data were collected on a Bruker APEXII diffractometer at 120 K. The structure was solved by direct methods and expanded using Fourier techniques. All non-hydrogen atoms were refined anisotropically and the refinement was carried out with full-matrix least-squares on *F*. All calculations were performed using the Yadokari-XG crystallographic software package. In the structure refinement, we could not determine the exact positions of the solvent molecules of crystallization because of their severe disorder. Their contribution was thus subtracted from the diffraction pattern by the "Squeeze" program.[2] Crystallographic data for $[Ru^{II}Cl(PY5Me_2)](PF_6)$: $C_{29}H_{25}ClN_5Ru{\cdot}PF_6$, FW = 725.03, yellow, Orthorhombic, space group *Pbcm*, cell parameters: a = 8.979(7) Å, b = 17.188(13) Å, c = 20.521(15) Å, V = 3167.0 (4) $Å^3$, T = 120 K, Z = 4, D_{calcd} = 1.521 g cm^{-3}, R_1 = 0.0359 ($I > 2\sigma(I)$) and wR_2 = 0.0859 (all the reflections), GOF = 1.138. CCDC-1022568 contains the supplementary crystallographic data.

Kinetic Studies on Oxidation Reactions with the Ru^{III}-OH Complex.

The Ru^{III}-OH complex **2** (0.5 mM) were generated in B.-R. buffer (pH 1.8) from the corresponding Ru^{II}-aqua complex, **1**. To the solution of **2**, was added a substrate (hydroquinone (H_2Q), 2-chloro-hydroquinone (H_2QCl), 2-fluoro-hydroquinone (H_2QF), ascorbic acid (AS), 2,5-chlorohydroquinone (H_2QCl_2), 2,3,5,6-tetrafluoro-hydroquinone (H_2QF_4), or 2-Methoxyhydroquinone ($H_2Q(OMe)$) with various concentrations at various temperatures in B.-R. buffer or deaturated B.-R. buffer. The reaction profiles were monitored by the rise of the absorption assigned to the resulting Ru^{II}-aqua complex, **1**, at 380 nm to determine the pseudo-first-order rate constants (k_{obs} / s^{-1}).

The saturation behaviours of the k_{obs} values were analysed by using following equation:[3]

$$k_{obs} = kK[Sub]/(1 + K[Sub]) \quad (1)$$

where K (M^{-1}) is the equilibrium constant for the pre-equilibrium, k (s^{-1}) is the first-order rate constant, and [Sub] (M) is the concentration of substrate used. Plots of k_{obs} vs. [Sub] were fitted by eq. 1 to determine k and K values. The k and K values determined at various temperatures were used to provide corresponding Eyring and van't Hoff plots, respectively.

Determination of Bond-Dissociation Energy (BDE) of 1.

The BDE of Ru^{II}-OH_2 complex **1** to form **2** in water was calculated with following equation 2:[4]

$$\text{BDE (kcal/mol)} = 1.37\ pK_a + 23.06\ E_{1/2} + 55.8 \qquad (2)$$

where pK_a is for the equilibrium between Ru^{II}-OH_2 (**1**) and its deprotonated form (Ru^{II}-OH^-) and $E_{1/2}$ (V vs SCE) is the redox potential of **1** to the corresponding Ru^{III}-OH_2 complex.

Marcus Plot for Electron-Transfer Oxidation of Hydroquinones with 2.

The curve fit of the rate constants for oxidation of the three substrates, shown in Fig 5, was done by using following eq 3:[5]

$$k_{ET} = (4\pi^3/h^2\lambda k_B T)^{1/2} V^2 \exp[-(\Delta G_{ET} + \lambda)^2/(4\lambda k_B T)] \qquad (3)$$

where V (cm^{-1}) is the electronic coupling matrix element, k_B (m^2 kg s^{-2} K^{-1}) is the Boltzman constant, h (m^2 kg s^{-1}) is the Planck constant, T (K) is the absolute temperature, ΔG_{ET} (eV) is the free energy change of electron transfer, and λ (eV) is the reorganization energy of electron transfer.

References.

1 Ünal, E. A.; Wiedemann, D.; Seiffert, J.; Boyd, J. P.; Grohmann, A. *Tetrahedron. Lett*. **2012**, *53*, 54.

2 P. V. D. Sluis and A. L. Spek, *Acta Crystallogr*., 1990, **A46**, 194.

3 Lam, W. W. Y.; Lau, T.-C. *Inorg. Chem*. **2006**, *45*, 315.

4 Bordwell, F. G.; Cheng, J.-P.; Ji, G.-Z.; Satish, A. V.; Zhang, X. *J. Am. Chem. Soc*. **1991**, *113*, 9790.

5 Marcus, R. A.; Sutin, N. *Biochim. Biophys. Acta* **1985**, *811*, 265.

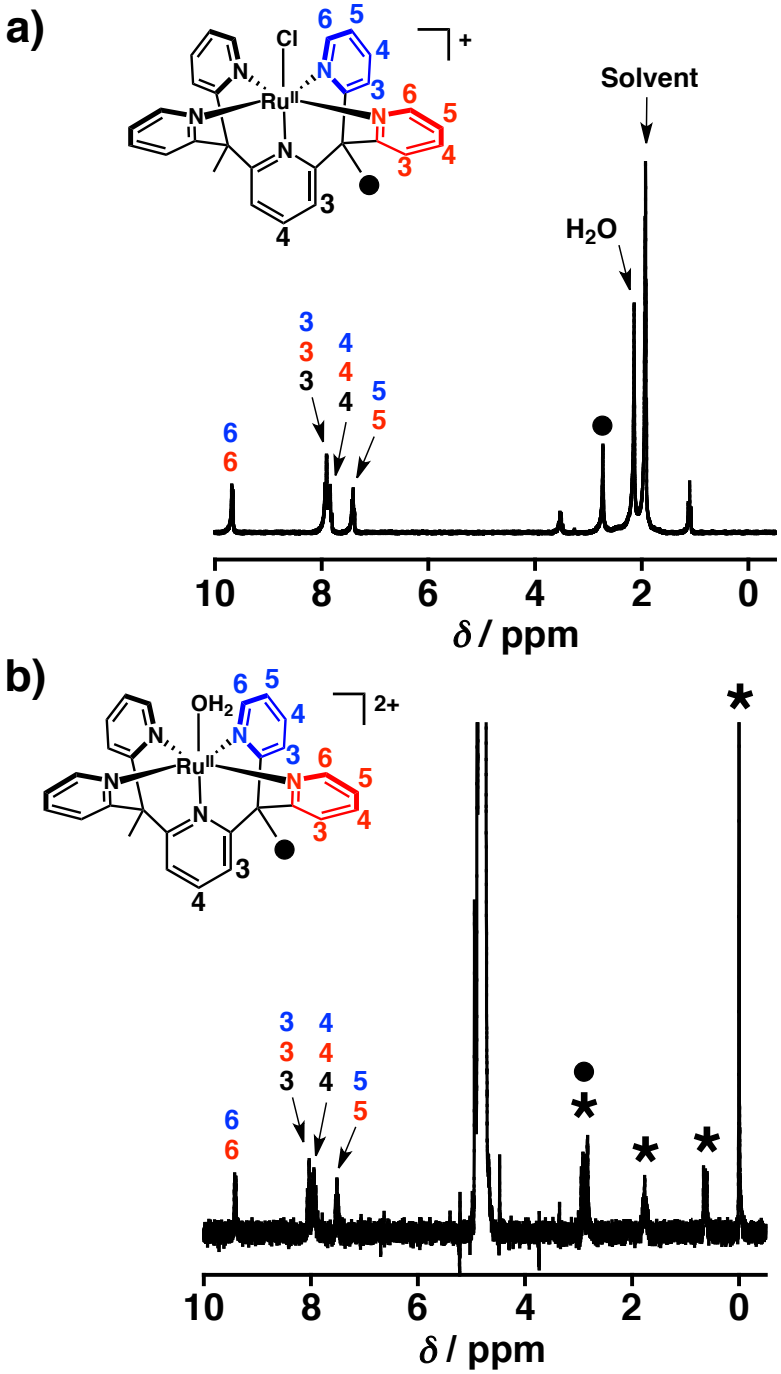

Fig. S1 ^{1}H NMR spectra of [RuCl(PY5Me$_2$)](PF$_6$) in CD_3CN (a) and **1** in B.-R buffered D_2O in the presence of 4,4-dimethyl-4-silapentane-1-sulfonic acid as an internal standard (b).

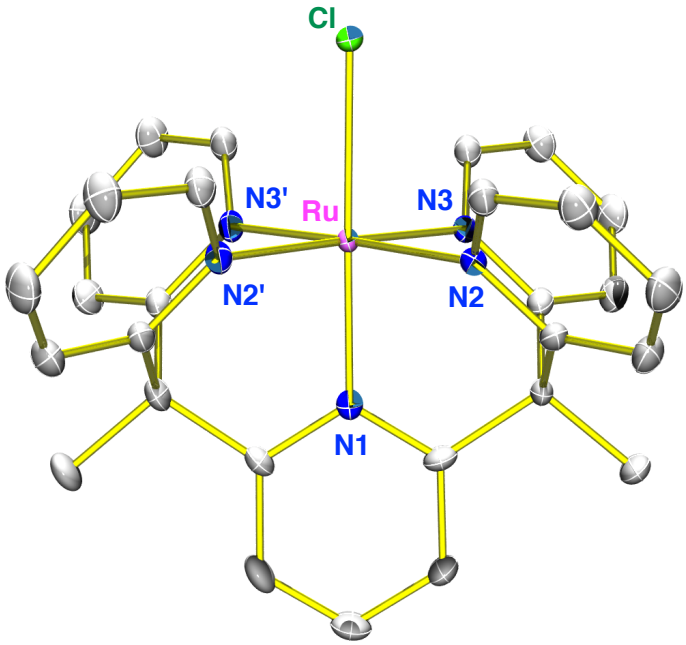

Fig. S2 ORTEP drawing of the cationic part of $[Ru^{II}Cl(PY5Me_2)](PF_6)$ with 50% thermal probabilities. The hydrogen atoms were omitted for clarity.

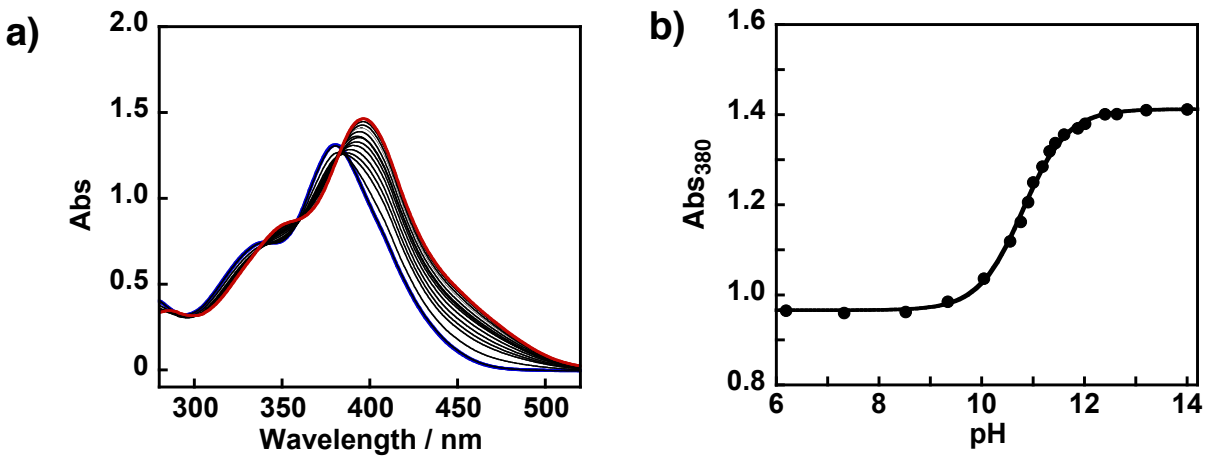

Fig. S3 The spectral changes during pH titration of **1** in B.-R. buffer (sample concentration: 1 mM) at room temperature: the pH range of 6.0–14.2 (a) and the plot of the absorbance change at 380 nm.

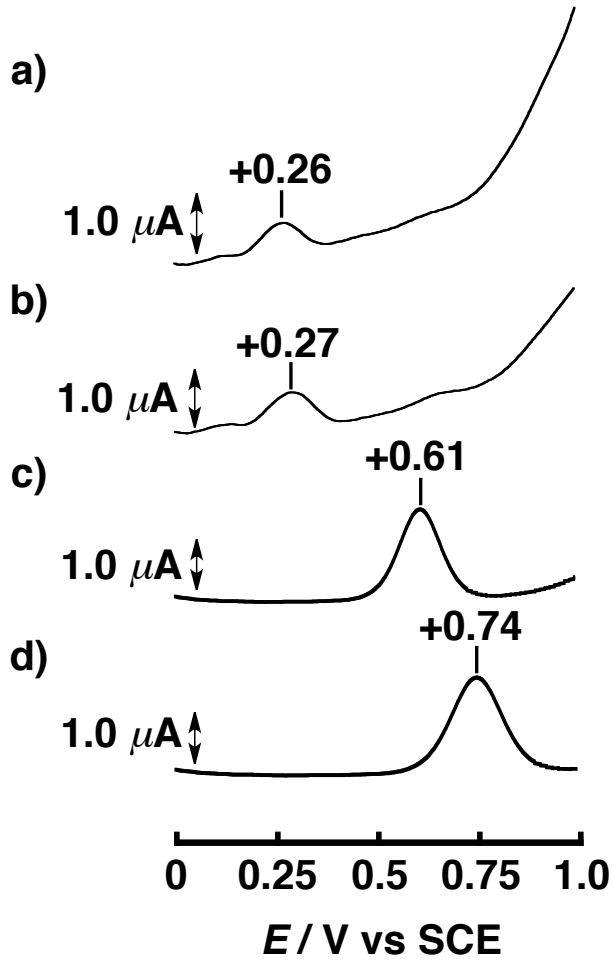

Fig. S4 Differential pulse voltammograms of **1** (0.5 mM) in B.-R. buffer at pH 2.12 (a), pH 4.55 (b), pH 11.30 (c), and pH 12.20 (d) at room temperature.

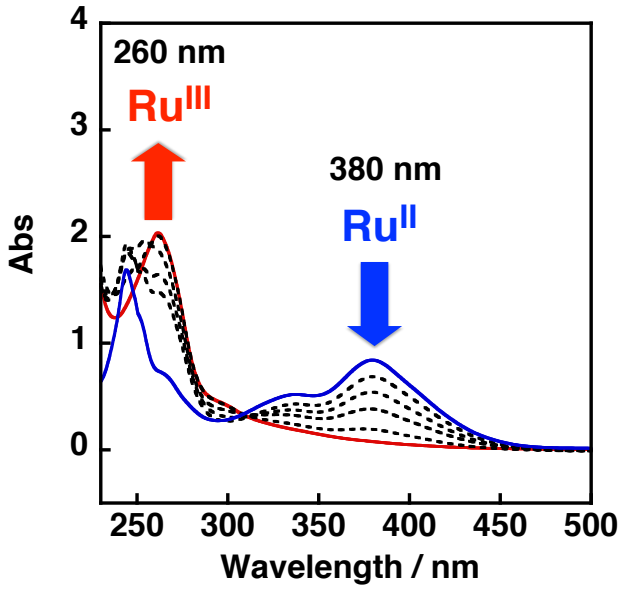

Fig. S5 Spectral changes at every 5 min during the electrochemical oxidation (at +1.3 V vs SCE) of **1** in B.-R. buffer (pH 1.8, sample concentration: 0.5 mM) at room temperature. The initial and the final spectra are indicated as the blue and red lines, respectively.

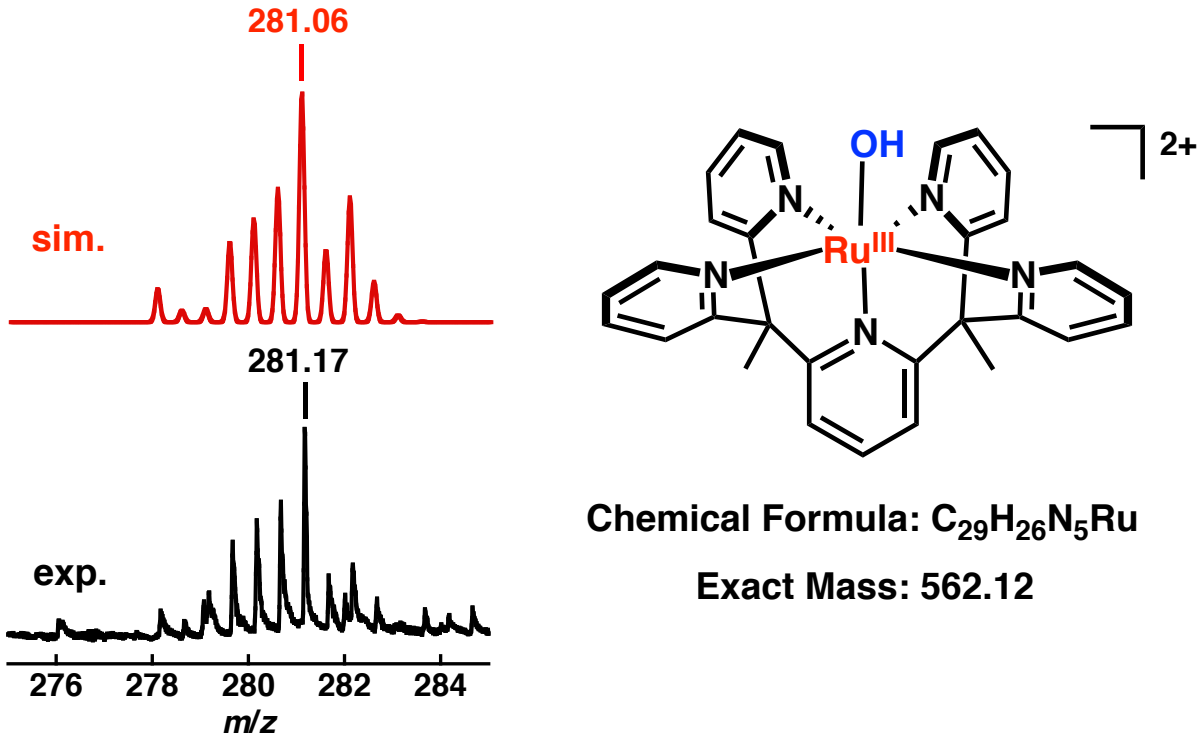

Fig. S6 ESI-MS spectrum of the aqueous solution of **2** (pH 1.8) generated by the electrochemical oxidation of **1** (below, black) and the computer simulation (above, red).

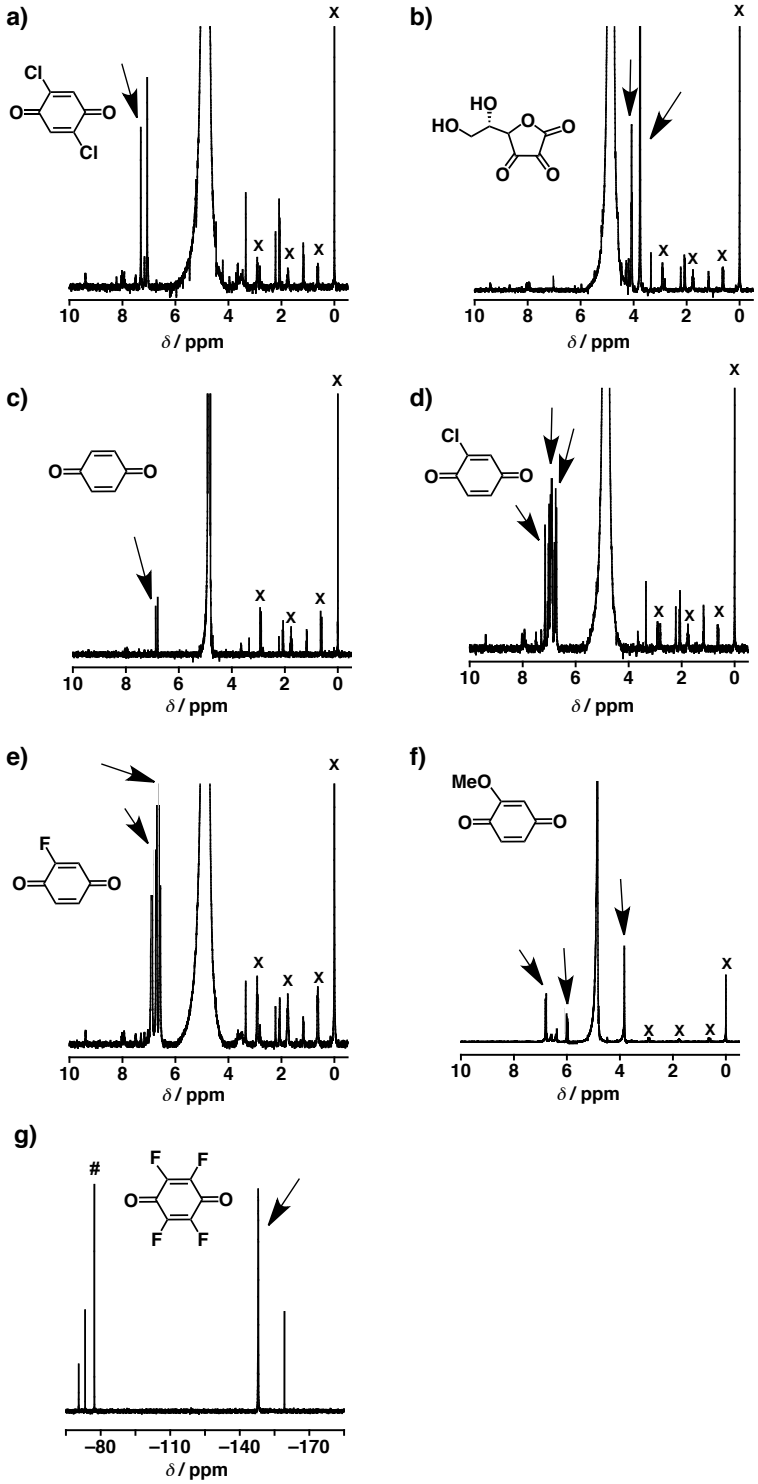

Fig. S7 ^{1}H NMR spectra of reaction mixtures derived from oxidations of H_2QCl_2 (a), AS (b), H_2Q (c), H_2QCl (d), H_2QF (e), and $H_2Q(OMe)$ (f), and ^{19}F NMR spectrum of that of H_2QF_4 (g) as substrates (1 μmol) in the presence of **2** (1 μmol) as the oxidant in D_2O. Arrows indicate the signals of each oxidation product. *: DSS as an internal reference. #: KF as an internal reference.

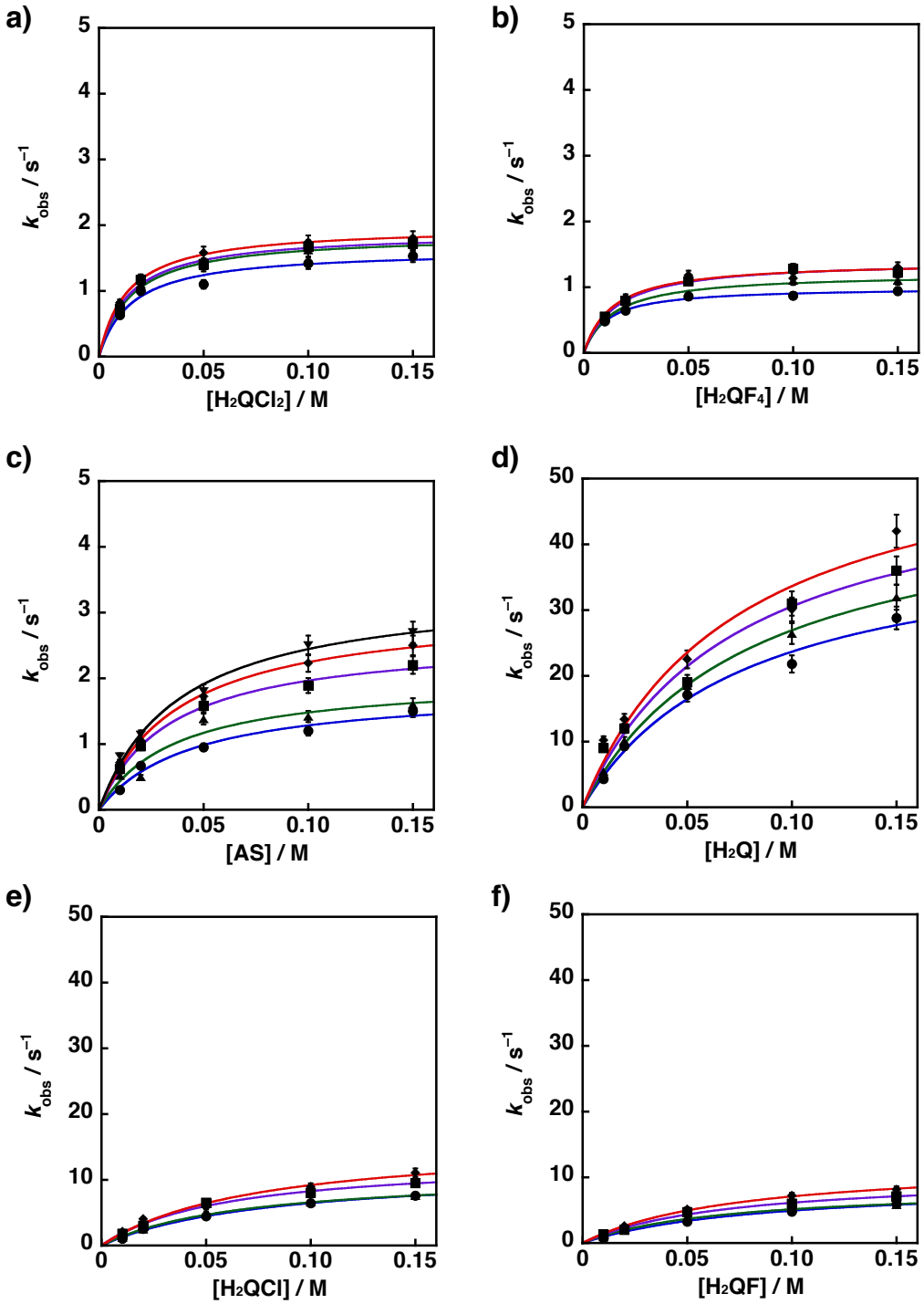

Fig. S8 Pseudo-first-order kinetic analysis for oxidation of substrates with complex **2** as oxidant (0.5 mM) in B.-R. buffer (pH 1.8) at 305 K (red), 297 K (purple), 289 K (green), and 281 K (blue). The substrates were H_2QCl_2 (a), H_2QF_4 (b), AS (c), H_2Q (d), H_2QCl (e), and H_2QF (f).

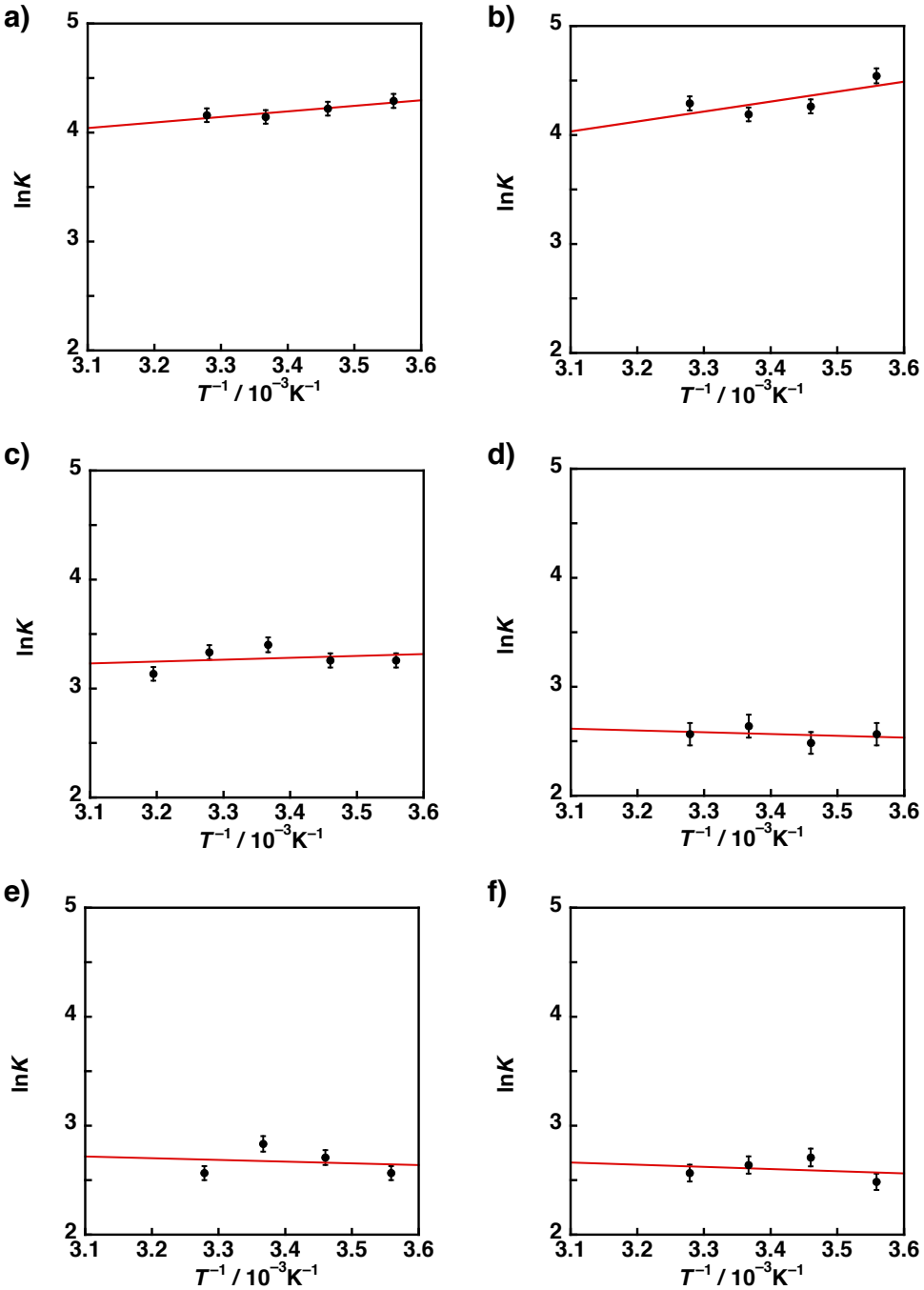

Fig. S9 van't Hoff plots for the pre-equilibrium processes for the substrate oxidation reactions using complex **2** (0.5 mM) in B.-R. buffer (pH 1.8). The substrates were H_2QCl_2 (a), H_2QF_4 (b), AS (c), H_2Q (d), H_2QCl (e), and H_2QF (f).

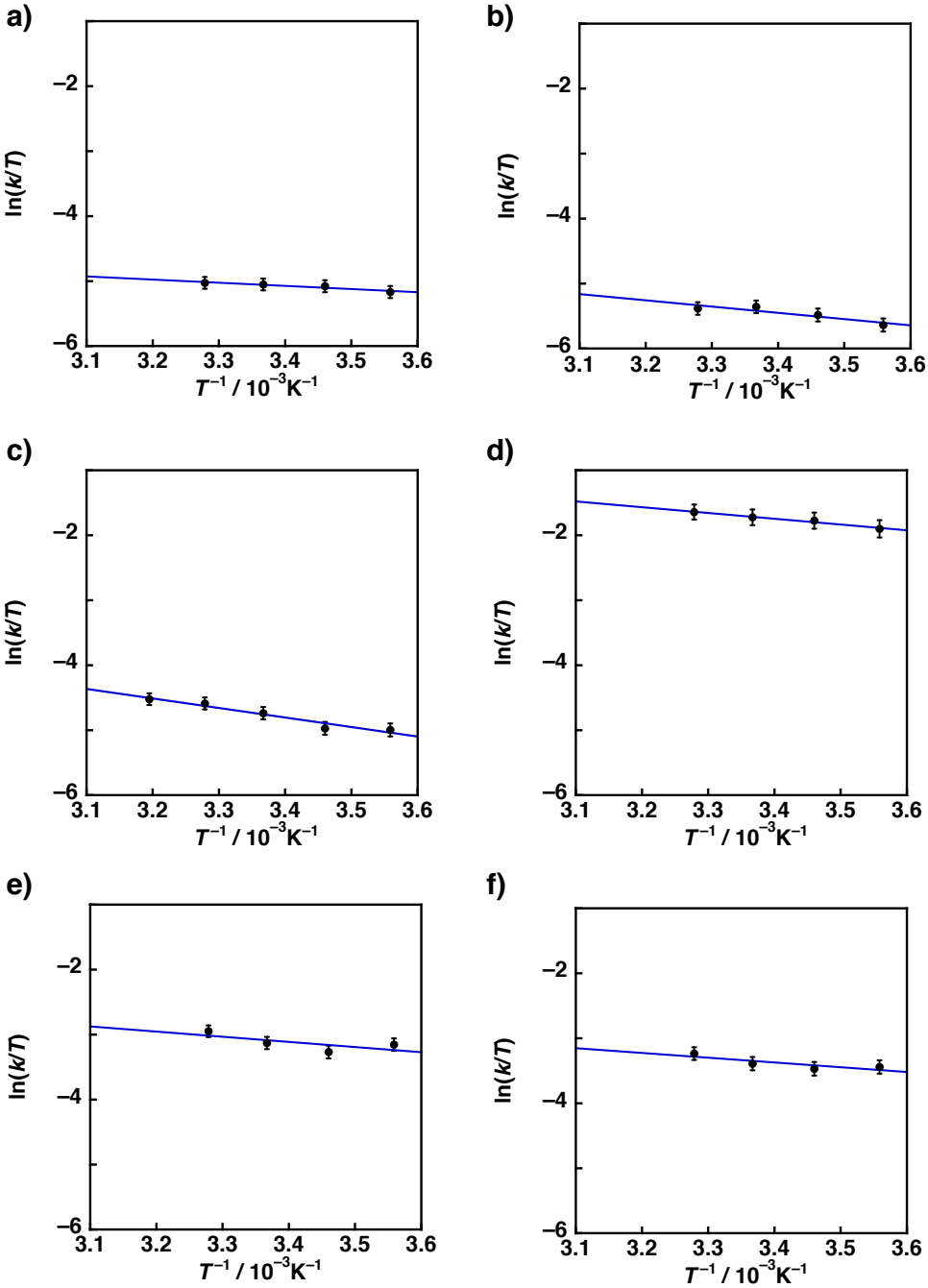

Fig. S10 Eyring plots for the substrate oxidation reactions using complex **2** (0.5 mM) in B.-R. buffer (pH 1.8). The substrates were H_2QCl_2 (a), H_2QF_4 (b), AS (c), H_2Q (d), H_2QCl (e), and H_2QF (f).

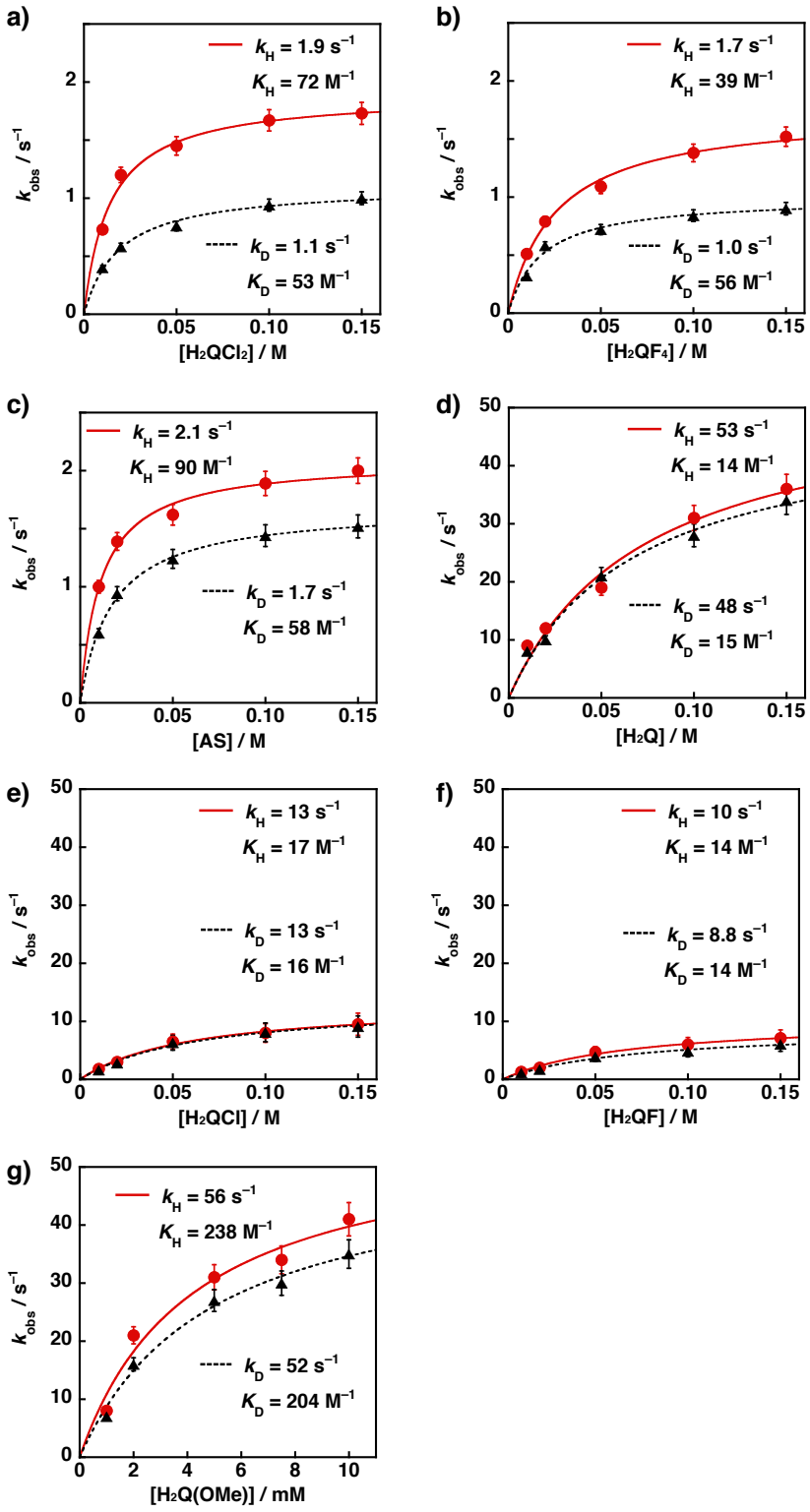

Fig. S11 Dependence of rate constants against substrate concentration for the oxidation of substrates with **2** in B.-R. buffer (pH 1.8) (red) and deaturated B.-R. buffer (pD 1.8) (black) at 297 K. The substrates were H_2QCl_2 (a), H_2QF_4 (b), AS (c), H_2Q (d), H_2QCl (e), H_2QF (f) and $H_2Q(OMe)$ (g).

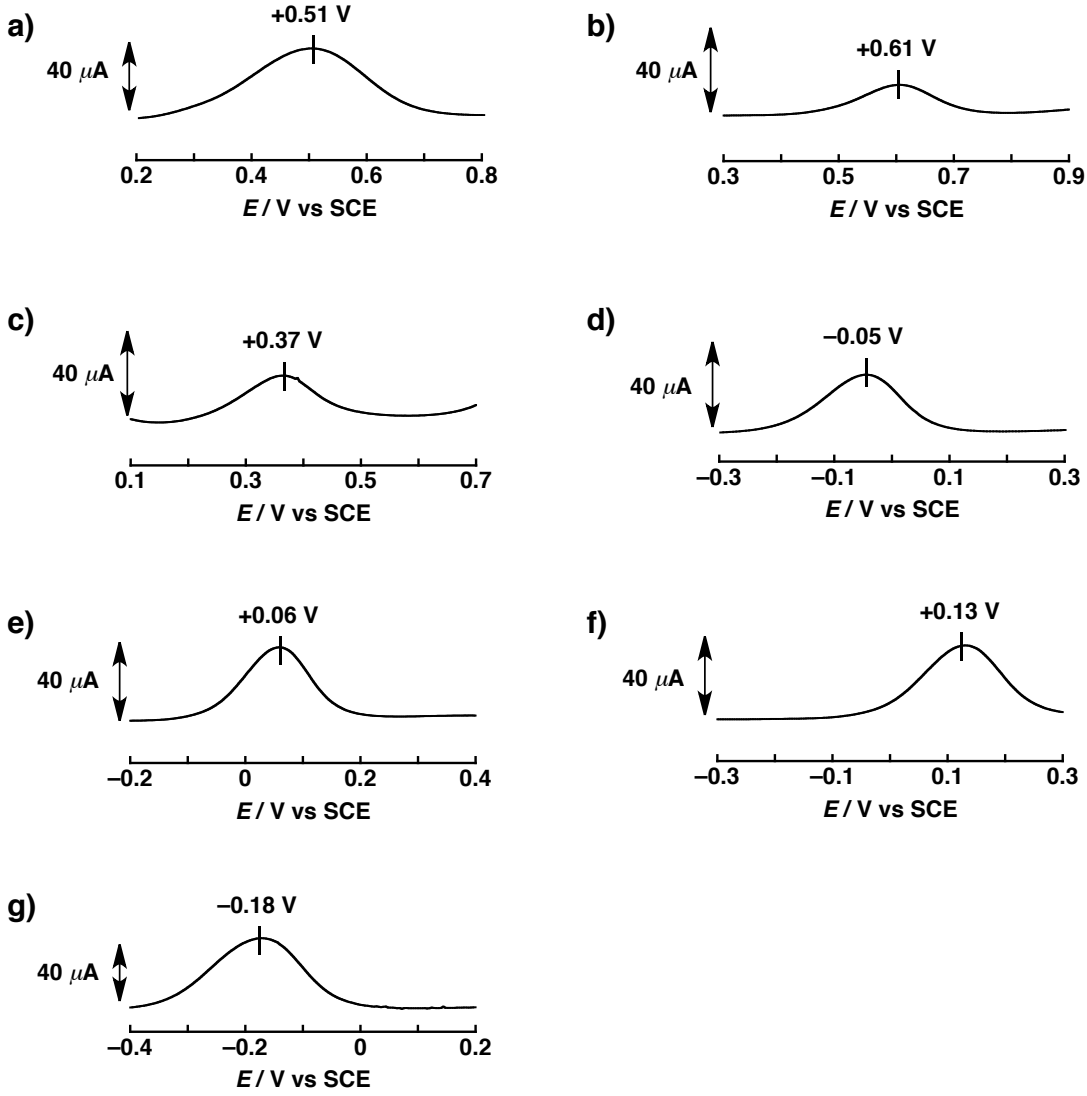

Fig. S12 Differential pulse voltammograms of substrates (1.0 mM) in B.-R. buffer (pH 1.8) at room temperature. The substrates were H_2QCl_2 (a), H_2QF_4 (b), AS (c), H_2Q (d), H_2QCl (e), H_2QF (f) and $H_2Q(OMe)$ (g).

Table S1 One-electron oxidation potentials (E_{ox}) of hydroquinone derivatives, driving forces of ET ($-\Delta G_{ET}$), ET rate constants (k_H) in ET and HAT reactions from hydroquinone derivatives to **2** at 298 K.

electron donor	E_{ox}, V *vs.* SCE	$-\Delta G_{ET}$, eV	k_H, s^{-1}
H_2QF_4	+0.61	0.14	1.7
H_2QCl_2	+0.51	0.24	1.9
AS	+0.37	0.38	2.1
H_2QF	+0.13	0.62	10
H_2QCl	+0.06	0.69	13
H_2Q	–0.05	0.80	53
$H_2Q(OMe)$	–0.18	0.93	56